Polymer Chemistry

Increased block copolymer length improves intracellular availability of protein cargo

Journal:	*Polymer Chemistry*
Manuscript ID	PY-ART-01-2022-000017.R1
Article Type:	Paper
Date Submitted by the Author:	24-Feb-2022
Complete List of Authors:	Hango, Christopher; University of Massachusetts, Department of Polymer Science and Engineering Davis, Hazel; University of Massachusetts, Department of Polymer Science and Engineering Uddin, Esha; University of Massachusetts, Department of Polymer Science and Engineering Minter, Lisa; University of Massachusetts, Department of Veterinary and Animal Sciences Tew, Gregory; University of Massachusetts, Department of Polymer Science and Engineering

Increased block copolymer length improves intracellular availability of protein cargo

Christopher R. Hango,[†] Hazel C. Davis,[†] Esha A. Uddin,[†] Lisa M. Minter,[‡,§] and Gregory N. Tew*[,†,‡,§]

[†]*Department of Polymer Science & Engineering, University of Massachusetts, Amherst, Massachusetts 01003, United States*

[‡]*Molecular and Cellular Biology Program, University of Massachusetts, Amherst, Massachusetts 01003, United States*

[§]*Department of Veterinary & Animal Sciences, University of Massachusetts, Amherst, Massachusetts 01003, Untied States*

Abstract

Amphiphilic protein transduction domain mimics (PTDMs) ranging from 15 to 120 repeat units in length were studied for their abilities to non-covalently bind and deliver proteins into Jurkat T cells. While shorter PTDMs facilitated greater EGFP and IgG internalization, longer block copolymers promoted heightened activity of Cre recombinase post-delivery, editing up to 60% of cells. Higher cargo activity devoid of higher cellular internalization implies that longer PTDMs improve the intracellular availability (IA) of the cargo, that is, the fraction of native protein successfully delivered and released at the target site. Dynamic light scattering of PTDM:IgG complexes revealed that increasing the carrier to cargo ratio yielded progressively larger aggregates with the shortest PTDM (up to ~1 μm), but no change in complex size with the longest amphiphile (~50 nm). Thus, employing longer PTDMs for protein delivery may be a useful tool for stabilizing non-covalent complex size, particularly given that smaller nanoparticles correlated with enhanced cargo activity.

Keywords

Block copolymer; protein delivery; polymer length; degree of polymerization; intracellular availability

Introduction

Formation of polymer-protein complexes via non-covalent interactions offers distinct advantages over covalent carrier-cargo attachment. In particular, such assemblies can be formed via a simple mixing step, analogous to polyplex formation in nucleic acid delivery, which circumvents the need for laborious coupling and purification steps.[1–3] Moreover, polymer-protein conjugation must typically be performed under mild aqueous conditions, greatly limiting the available synthetic routes, and frequently leads to substantial reduction in protein activity.[1,4–7] Owing to the immense heterogeneity in composition, structure, and stability of proteins, successful strategies for conjugate preparation are also challenging to broadly apply to other protein cargoes. In contrast, non-covalent delivery offers flexibility in that carriers and cargoes can be easily substituted or combined in any proportion, enabling rapid screening of libraries for elucidation of structure-activity relationships. Polymer-protein complexes are distinct from other polymer nanoparticle systems, such as those employing carrier self-assembly (e.g., polymeric micelles and polymersomes) or physical methods (e.g., nanoprecipitation and emulsions) to produce delivery vehicles. Instead, complexation is induced by strong carrier-cargo associations, including electrostatic, hydrophobic, and hydrogen bonding interactions.[2,8,9] Although the homogenous, colloidal aggregates formed by non-covalent complexation lack the precise order that is characteristic of self-assembling carrier systems, a wider range of polymeric structures can be employed, given that the ability to self-assemble is not a requirement.

While a number of natural and synthetic polymeric carriers have been reported to deliver proteins via complexation, optimization has focused largely on chemical modifications rather than degree of polymerization (DP).[3,10,11] Prominent examples in which DP has been explicitly modulated in the context of protein complexation and delivery have primarily focused on cationic homopolymers of chitosan[12–17] and polyethylenimine (PEI)[18,19] complexed with model proteins, such as bovine serum albumin (BSA), human serum albumin (HSA), and insulin. The cationic nature of both chitosan and PEI enables strong interactions with anionic cargoes and cellular membranes, making them popular choices for a range of delivery applications. Although not applied to intracellular delivery, the effect of molecular weight on BSA and HSA complexation by hydrophobically-modified poly(ethylene glycol) (PEG) has also been investigated.[20] Altogether, these studies have explored polymer-protein binding, complex size, complex stability, protein release, and retention of protein structure and activity as a function of polymer DP. Though results were sometimes conflicting, longer polymers generally appeared to strengthen carrier-cargo interactions and retard protein release at the cost of increasingly altered protein conformation.[12,14–16,19,20] The effects of DP on block copolymer-protein complexation are severely understudied. Block copolymers typically combine disparate chemical properties, resulting in fundamentally different interactions with both proteins and lipid membranes. In particular, lengthening amphiphilic block copolymers would be expected to increase their surfactant-like character, potentially giving rise to self-assembly, cargo denaturation, enhanced endosomal escape, or increased cellular toxicity.[21–25]

Several of these interdependent effects can be condensed into a single parameter which is more practically measured, the cargo's intracellular availability (IA). IA is defined as the fraction of total delivered cargo which reaches its intracellular target without loss of function and serves to

summarize the post-internalization capacity of a cargo to perform its intended biological function.[26–29] High IA requires the carrier not only to transduce the plasma membrane and distribute within the correct subcellular compartment, but also to protect the cargo from degradation or denaturation during transport and facilitate its release upon reaching the target site (Figure 1).[6] Although absolute measurements of the numerator and denominator of IA are virtually impossible to achieve, indirect or relative tools can be adequately employed, such as fluorescence-based assays or downstream readouts of protein function, as demonstrated here and in a recent report.[29] In this way, the impacts of carrier structure on both cargo uptake and function can be better understood and used to inform the design of the next generation of delivery vehicles.

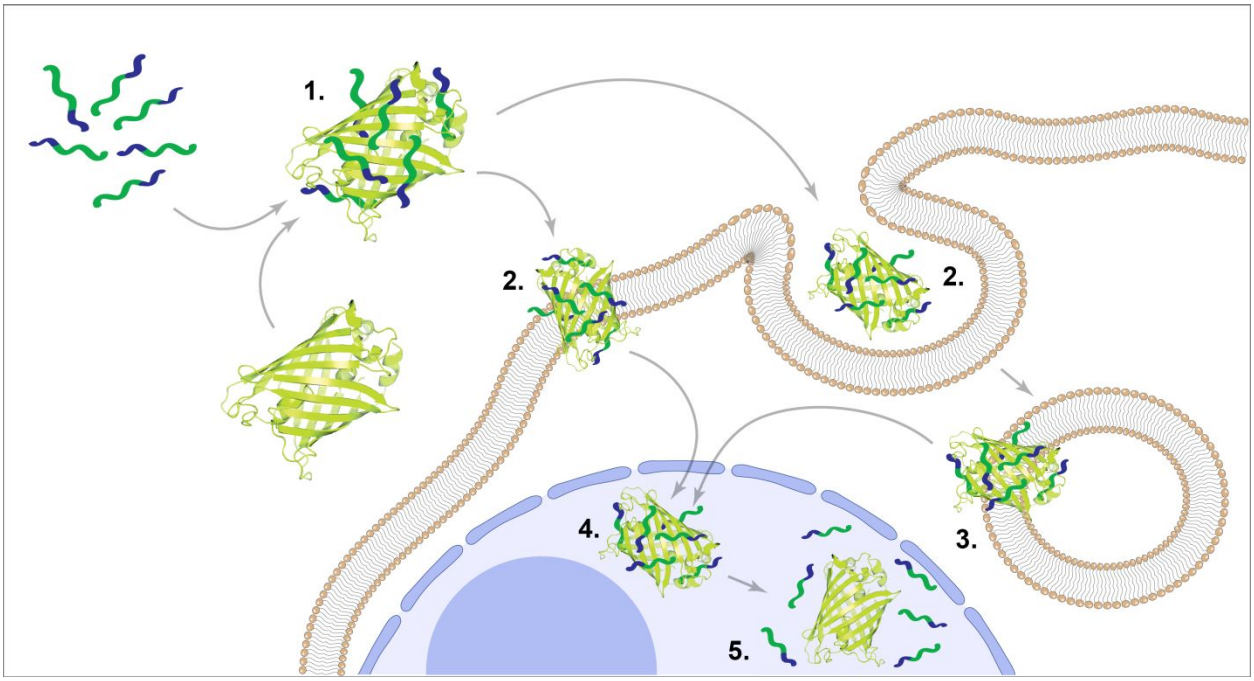

Figure 1: Bottlenecks in the non-covalent delivery landscape which can impede a cargo's intracellular availability: (1) carrier-cargo association, (2) cellular internalization via endocytosis or direct translocation, (3) endosomal escape, (4) subcellular localization, and (5) cargo release.

Our group has developed a library of synthetic guanidine-rich polymers known as protein transduction domain mimics (PTDMs) which resemble the membrane-transducing peptide sequences found in HIV-1 Tat and Antennapedia.[30–34] The effects of DP and charge density on

siRNA delivery have been thoroughly explored using both cationic homopolymers and cationic-hydrophobic block copolymers, however, such optimization has thus far not been extended to protein delivery.[35–37] To date, ring-opening metathesis polymerization-based PTDMs have been used at a maximum length of just 20 repeat units with protein cargoes.[38,39]

Block copolymer PTDMs have consistently outperformed their homopolymer counterparts for protein delivery, likely due to insufficient hydrophobicity and poor cargo binding of homopolymers.[9,29,38,40,41] However, the aforementioned studies employing chitosan, PEI, and PEG homopolymers suggest that lengthening PTDM homopolymers may similarly enhance carrier-cargo binding, preserve native protein structure, and ultimately boost internalization. Likewise, there is motivation to understand the impact of PTDM charge density on protein delivery.[16] Accordingly, PTDMs comprising 20-60 repeat units with charge densities of one or two guanidinium groups per monomer (7-22 kDa and 12-35 kDa in size, respectively) have been studied here for EGFP delivery. Past optimization of block copolymers indicated that incorporation of hydrophobic and hydrophilic monomers at a 2:1 ratio maximizes both protein internalization and function.[39,42] Additionally, PTDMs constructed from a hydrophobic monomer featuring methyl and phenyl substituents (**MePh**) and a cationic monomer containing two guanidine groups (**dG**) have demonstrated robust delivery of several functional proteins, including antibodies and enzymes.[29,42–46] Maintaining a 2:1 ratio of **MePh** to **dG**, four new carriers were synthesized with DPs of 15-120 (6-46 kDa in size). This series of block copolymers was used here to deliver EGFP, IgG, and Cre recombinase to elucidate the impact of molecular weight on both internalization and protein activity.

Results

Polymer Design

In an effort to isolate the effects of polymer length and charge density on protein delivery, homopolymers were synthesized with targeted DPs of 20, 40, and 80 repeat units, containing either one (poly[guanidinium oxanorbornene], or **PGON**) or two (diGuanidine, or **dG**) positive charges (Scheme 1). Given the well-established importance of hydrophobicity in non-covalent protein delivery, a series of block copolymers were synthesized consisting of a hydrophobic block (featuring methyl and phenyl substituents, or **MePh**) and a cationic block (**dG**).[1,29,38,40,41] These carriers were designed to contain a 2:1 ratio of hydrophobic to cationic repeat units (**MePh$_{2n}$-*b*-dG$_n$**) at DPs of 15, 30, 45, 60, and 120 (*2n*/*n* = 10/5, 20/10, 30/15, 40/20, and 80/40) to assess the impact of carrier length on both cargo uptake and biological activity.

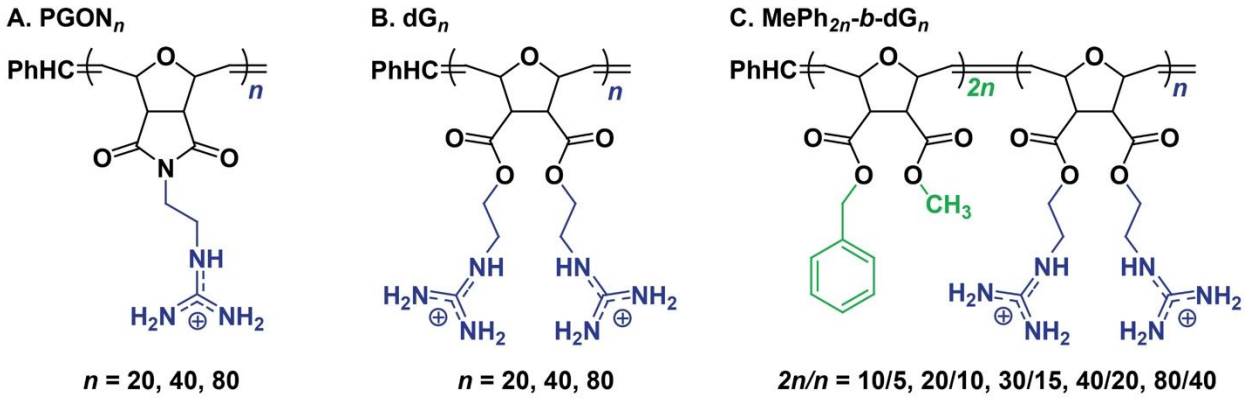

Scheme 1: Protein transduction domain mimic (PTDM) carriers comprising various charge densities, macromolecular architectures, and chain lengths. (A) Poly(guanidinium oxanorbornene) (**PGON$_n$**) homopolymers featuring one cationic charge per repeat unit. (B) Diguanidine (**dG$_n$**) homopolymers containing two cationic charges per repeat unit. (C) Block copolymers of hydrophobic (methyl/phenyl substituents, green) and cationic (guanidine substituents, blue) monomers incorporated at a constant 2:1 ratio (**MePh$_{2n}$-*b*-dG$_n$**). **PGON$_n$**, **dG$_n$**, and **MePh$_{2n}$-*b*-dG$_n$** homopolymers consisted of 20-80 repeat units (20-80 and 40-160 cationic charges per polymer for the **PGON$_n$** and **dG$_n$** series, respectively), while block copolymers were synthesized with 15-120 repeat units (10-80 cationic charges).

Homopolymer-Mediated Protein Internalization

Homopolymers were complexed with 60 nM EGFP and incubated with Jurkat T cells for 4 hours to allow for cellular internalization (Figure 2). In much the same way that N:P ratio is been held constant when optimizing the length of polymeric carriers for nucleic acid delivery, the ratio of polymer repeat units to protein molecules was maintained at 400:1 for all carriers.[35,37] As a result, the number of polymer chains in the system was decreased with increasing polymer length, effectively isolating the effect of monomer connectivity on carrier performance.

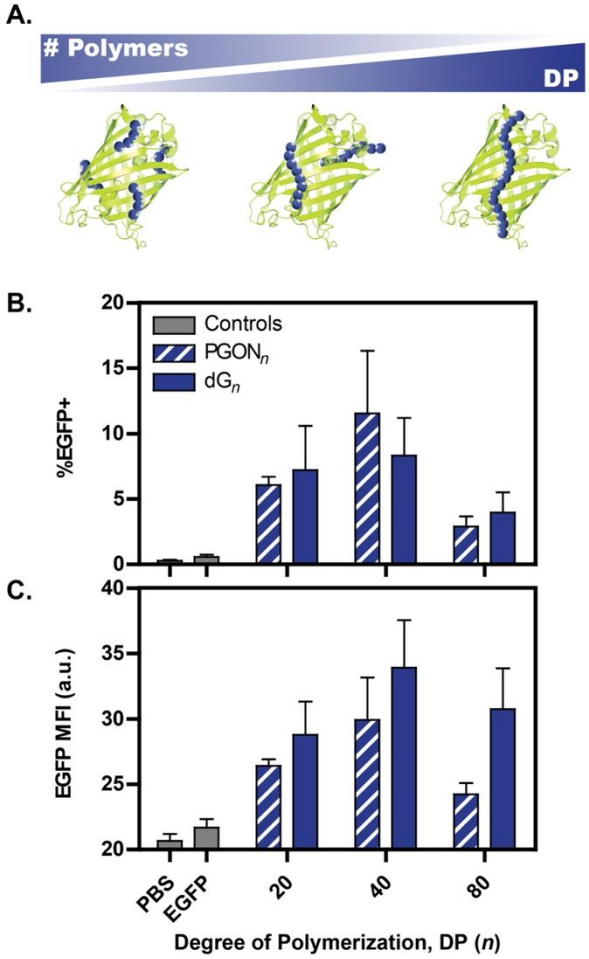

Figure 2: EGFP internalization in Jurkat T cells as a function of both homopolymer PTDM degree of polymerization (DP) and cationic charge density. (A) Illustration of the inverse relationship between DP and number of polymer molecules in the system given that the total number of polymer repeat units in the system is universally conserved. As shorter polymers are linked together to form longer ones, fewer independent chains remain, allowing for a direct assessment of the impact of monomer connectivity on delivery. The impact of charge density is observed by

comparing polymers with one (hatched blue bars) and two (solid blue bars) charges per repeat unit at equal DPs (each pair of adjacent bars). EGFP internalization is quantified as (B) percentage of live cells positive for EGFP and (C) median fluorescence intensity (MFI) of the entire live-cell population. Data are displayed as the mean ± the standard error of the mean for four independent replicates of 10,000 cells each. Statistical analysis of the dataset was done by one-way ANOVA followed by a Tukey post-test. For all samples, p values were > 0.05 when compared to the PBS and EGFP controls (grey).

EGFP internalization was assessed by flow cytometry using two metrics: percentage of the cellular population positive for cargo in any quantity and median EGFP fluorescence intensity (MFI) of the population, a measure of quantity delivered per cell. Not unlike past siRNA studies, both metrics suggested marginally better delivery with polymers of intermediate length, however, the differences here were insignificant owing to consistently poor internalization by all carriers.

Block Copolymer-Mediated Internalization and Activity

In a similar experiment, delivery of 50 nM EGFP was compared using three lengths of **MePh$_{2n}$-*b*-dG$_n$** carriers at a ratio of 600 polymer repeat units per protein (Figure 3). In sharp contrast with homopolymer-mediated delivery, the shortest polymer facilitated EGFP internalization in virtually the entire cell population, while the longer two polymers failed entirely.

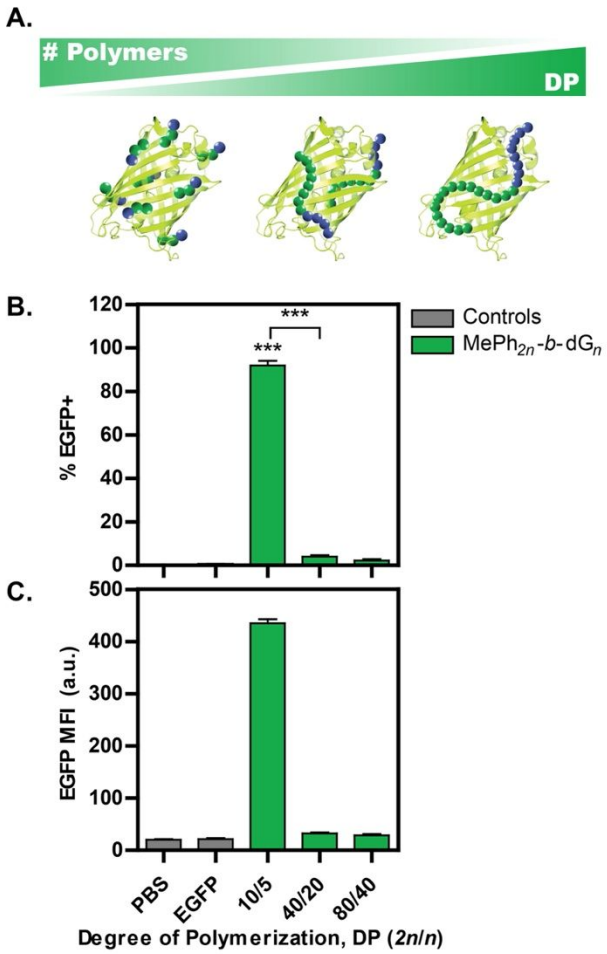

Figure 3: EGFP internalization in Jurkat T cells as a function of block copolymer PTDM degree of polymerization (DP). (A) Illustration of the inverse relationship between DP and number of polymer molecules in the system given that the total number of polymer repeat units in the system is universally conserved. As shorter polymers are linked together to form longer ones, fewer independent chains remain, allowing for a direct assessment of the impact of monomer connectivity on delivery. EGFP internalization is quantified as (B) percentage of live cells positive for EGFP and (C) median fluorescence intensity (MFI) of the entire live-cell population. Data are displayed as the mean ± the standard error of the mean for three independent replicates of 10,000 cells each. Statistics indicate significance in comparison with the PBS and EGFP controls (grey), unless otherwise noted: * = $p < 0.05$, ** = $p < 0.01$, *** = $p < 0.001$, no symbol = no significance, as determined by one-way ANOVA followed by a Tukey post-test.

Although fluorescence is typically directly correlated with concentration of delivered protein, it is possible that the longer, more surfactant-like amphiphiles denatured EGFP, destroying its fluorophore. If true, lower fluorescence would be observed regardless of internalization level. To investigate this possibility, a second protein cargo was delivered, this time labelled with a small molecule dye whose fluorescence is independent of protein conformation. In this experiment, 50 nM of an AlexaFluor 488 conjugated antibody (IgG-AF488) was delivered into Jurkat T cells, this

time at a ratio of 300 polymer repeat units per protein (Figure 4). Similar to EGFP, IgG-AF488 internalization was significantly diminished when delivered with longer PTDMs. However, these longer polymers nonetheless delivered some IgG-AF488. This trend was replicated in a second cell line, embryonic mouse hippocampal-18 (mHippoE-18) cells (Figure S18).

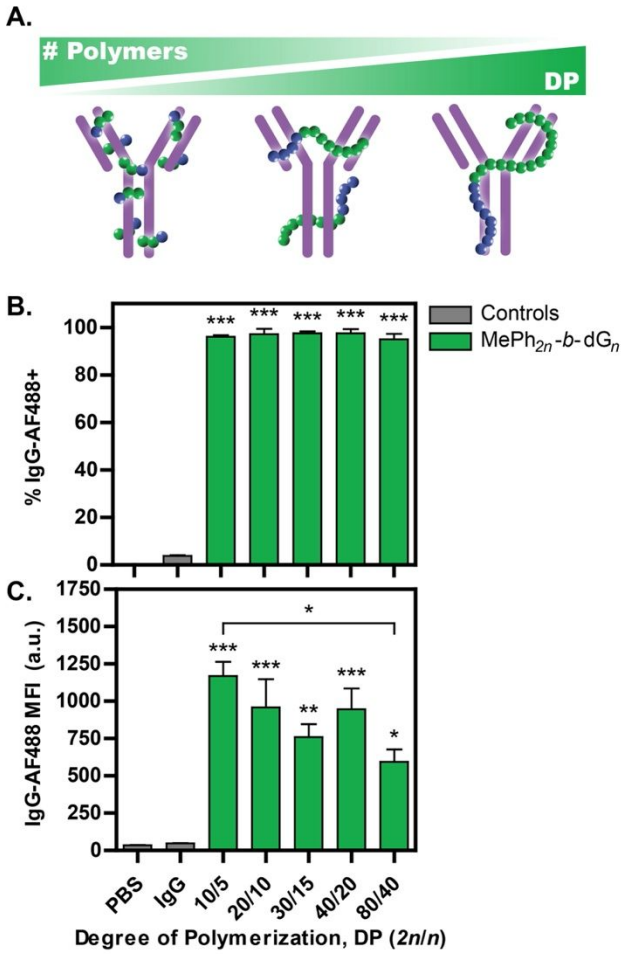

Figure 4: AlexaFluor (AF)488 conjugated IgG internalization in Jurkat T cells as a function of PTDM degree of polymerization (DP). (A) Illustration of the inverse relationship between DP and number of polymer molecules in the system given that the total number of polymer repeat units in the system is universally conserved. As shorter polymers are linked together to form longer ones, fewer independent chains remain, allowing for a direct assessment of the impact of monomer connectivity on delivery. IgG internalization is quantified as (B) percentage of live cells positive for AF488 and (C) median fluorescence intensity (MFI) of the entire live-cell population. Data are displayed as the mean ± the standard error of the mean for four independent replicates of 10,000 cells each. Statistics indicate significance in comparison with the PBS and IgG controls (grey), unless otherwise noted: * = $p < 0.05$, ** = $p < 0.01$, *** = $p < 0.001$, no symbol = no significance, as determined by one-way ANOVA followed by a Tukey post-test.

As recently demonstrated with this PTDM system, high cargo activity can be achieved despite low internalization.[29] That is, maximal internalization is not necessarily associated with heightened

cargo intracellular availability. For this reason, the block copolymer series was further screened for its ability to deliver a model bioactive cargo, Cre recombinase, into a reporter Jurkat T cell line at 125 nM protein and a ratio of 75 polymer repeat units per protein (Figure 5). On-target delivery of structurally uncompromised Cre resulted in recombination of the *EGFP* gene and subsequent loss of cellular fluorescence. In stark contrast with internalization experiments, maximal protein activity was achieved with the longest carriers, **MePh$_{40}$-*b*-dG$_{20}$** and **MePh$_{80}$-*b*-dG$_{40}$**.

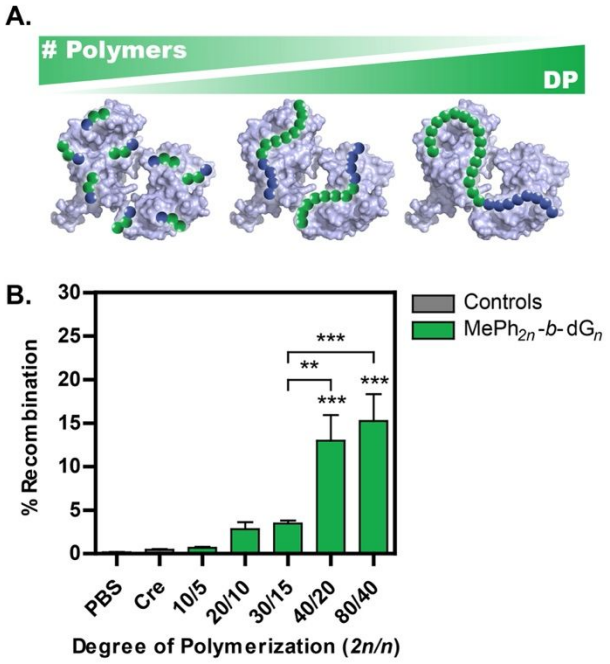

Figure 5: Functional delivery of Cre recombinase in Jurkat T cells, modified to express a floxed *EGFP* gene, as a function of PTDM degree of polymerization (DP). (A) Illustration of the inverse relationship between DP and number of polymer molecules in the system given that the total number of polymer repeat units in the system is universally conserved. As shorter polymers are linked together to form longer ones, fewer independent chains remain, allowing for a direct assessment of the impact of monomer connectivity on delivery. Functional Cre delivery is quantified as (B) percentage of cells negative for EGFP fluorescence 6 days post-delivery. Data are displayed as the mean ± the standard error of the mean for four independent replicates of 10,000 cells each. Statistics indicate significance in comparison with the PBS and Cre controls (grey), unless otherwise noted: * = $p < 0.05$, ** = $p < 0.01$, *** = $p < 0.001$, no symbol = no significance, as determined by one-way ANOVA followed by a Tukey post-test.

Although **MePh$_{80}$-*b*-dG$_{40}$** achieved the highest Cre activity at the conditions selected, the gene recombination rate was fairly low (~15%) in comparison with past studies using this cargo.[29,40,42,47] Given that increasing PTDM:Cre ratio has been shown to elevate activity, ratios between 0.625:1 and 5:1 (the ratios used for **MePh$_{80}$-*b*-dG$_{40}$** and **MePh$_{10}$-*b*-dG$_{5}$** in Figure 5, respectively) were

surveyed for the shortest and longest PTDMs (Figure 6).[47] Importantly, the ratio of polymer repeat units to protein molecules was not maintained in this case. Each new condition tested represented progressively lower (or higher) ratios for **MePh$_{10}$-*b*-dG$_5$** (or **MePh$_{80}$-*b*-dG$_{40}$**) compared to the ratio used in Figure 5. As expected, increasing polymer:protein ratio promoted higher gene recombination. It is worth noting, however, that at the highest mass of polymer used (i.e., **MePh$_{80}$-*b*-dG$_{40}$** with a 5:1 ratio), a slight drop in performance was observed. This reduction in activity coincided with severe cytotoxicity (~25% viable cells), suggesting that many of the cells receiving large quantities of protein did not survive.

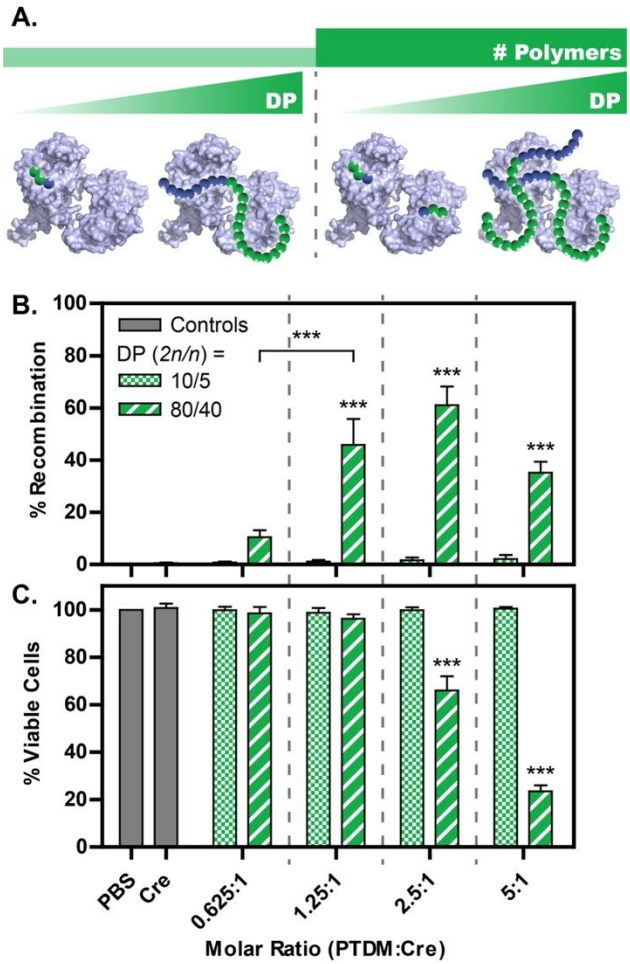

Figure 6: Functional delivery of Cre recombinase in Jurkat T cells, modified to express a floxed *EGFP* gene, as a function of both PTDM degree of polymerization (DP) and number of polymer chains in the system (i.e., molar ratio of PTDM:Cre). (A) Illustration of the experimental design, in which PTDMs with two different DPs (**MePh$_{10}$-*b*-dG$_5$** and **MePh$_{80}$-*b*-dG$_{40}$**) were studied at increasing ratios of PTDM chains to Cre molecules. Results are presented as

(B) percentage of cells negative for EGFP fluorescence 6 days post-delivery and (C) cellular viability immediately following delivery. Each pair of bars represents delivery at equal polymer chain concentration, but unequal polymer repeat unit concentration (**$MePh_{10}$-*b*-dG_5** << **$MePh_{80}$-*b*-dG_{40}**). Data are displayed as the mean ± the standard error of the mean for four independent replicates of 10,000 cells each. Statistics indicate significance in comparison with the PBS and Cre controls (grey), unless otherwise noted: * = $p < 0.05$, ** = $p < 0.01$, *** = $p < 0.001$, no symbol = no significance, as determined by one-way ANOVA followed by a Tukey post-test.

Block Copolymer-Mediated Binding and Particle Size

The dramatic differences in cargo functionality when delivered with different length PTDMs, particularly considering the contradictory trend when compared with internalization, prompted speculation that there may be similarly large physical disparities in the polymer:protein complexes. Carrier-cargo association strength was probed using a model protein cargo, BSA-FITC, in a previously-established fluorescence-based binding assay (Figure S26).[29,40,48,49] Cargo binding appeared to be driven by the polymer repeat unit to protein ratio (i.e., mass concentration of polymer in the system) rather than PTDM DP. This finding suggests that, in all experiments exploring the effect of increased monomer connectivity, proteins were bound with similar strengths by their carriers.

Dynamic light scattering (DLS) was subsequently used to probe the physical size of PTDM:IgG nanoparticles as a function of DP (Figure 7A-B and Figures S27-S28). Complex diameter decreased dramatically with increasing polymer length, from ~1 μm to 50 nm, equating to a reduction in particle volume of nearly four orders of magnitude, assuming a spherical morphology. DLS of PTDM:Cre complexes similarly revealed a drop in particle diameter from ~620 nm to 270 nm, corresponding to approximately an order of magnitude by volume (Figures S31-S33).

To gain more insight into the complex formation process, the shortest and longest polymers were further studied by DLS at two PTDM:IgG ratios, 2.5:1 and 20:1, spanning the range of ratios employed in IgG delivery (Figure 7C-D and Figures S29-S30). Consistent with previous findings,

MePh$_{10}$-*b*-dG$_5$:IgG nanoparticles grew substantially in size as more polymer was introduced into the system.[22,50] In contrast, **MePh$_{80}$-*b*-dG$_{40}$**:IgG nanoparticles remained the same ~50 nm size despite the eight-fold increase in polymer concentration.

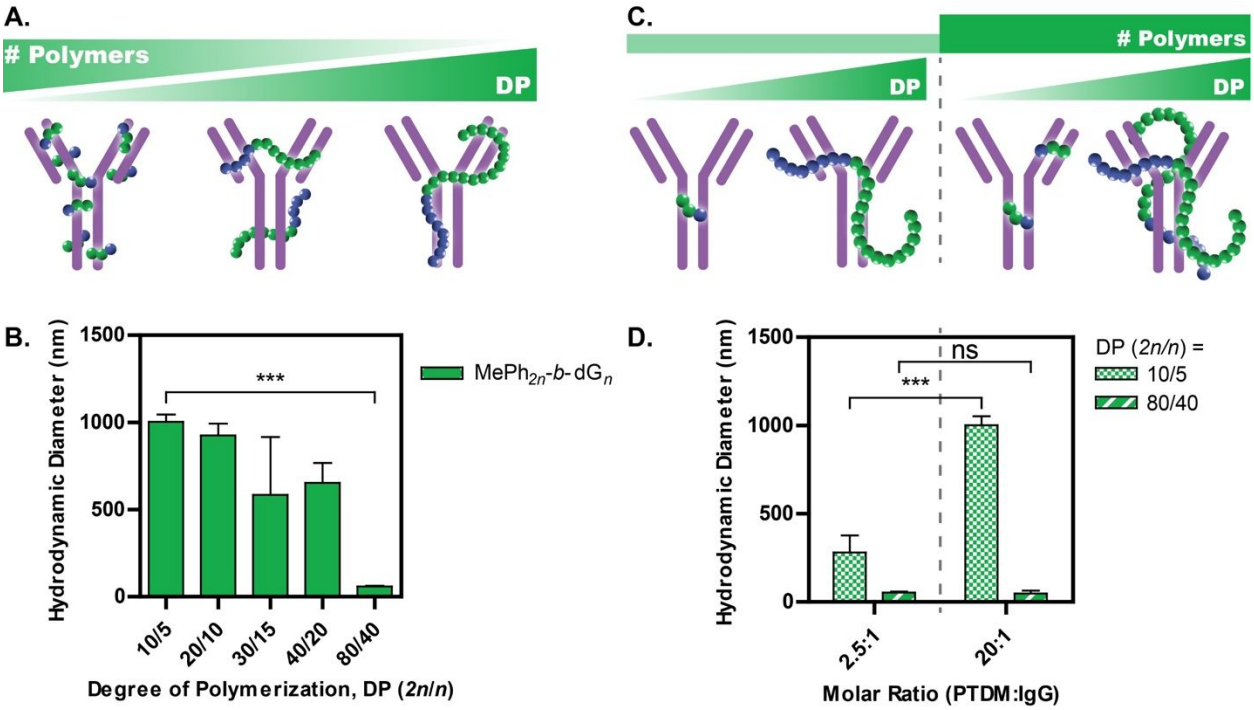

Figure 7: PTDM:IgG complex size as a function of (A-B) PTDM degree of polymerization (DP) and (C-D) number of polymer chains in the system (i.e., molar ratio of PTDM:IgG). (A) Illustration of the inverse relationship between DP and number of polymer molecules in the system in the first experiment, given that the total number of polymer repeat units in the system is universally conserved. As shorter polymers are linked together to form longer ones, fewer independent chains remain, allowing for a direct assessment of the impact of monomer connectivity on complex size. (B) PTDM:IgG complex diameter as measured by dynamic light scattering (DLS) for increasing PTDM DP. (C) Illustration of the second experimental design, in which PTDMs with two different DPs (**MePh$_{10}$-*b*-dG$_5$** and **MePh$_{80}$-*b*-dG$_{40}$**) were studied at increasing ratios of PTDM chains to Cre molecules. (D) PTDM:IgG complex diameter as determined by DLS, where each pair of bars represents complex size at equal polymer chain concentration, but unequal polymer repeat unit concentration (**MePh$_{10}$-*b*-dG$_5$** << **MePh$_{80}$-*b*-dG$_{40}$**). Data are presented as the mean size (by number) of the most populous distribution (when multimodal) ± the standard deviation for two (D) or three (B) independent replicates, each comprising three individual measurements of the same sample. In the case that a weak correlation curve was obtained, no meaningful data was obtained and the measurement was omitted. Further details regarding data analysis can be found in the Supporting Information. Statistics indicate significance between the two data points indicated by brackets: * = $p < 0.05$, ** = $p < 0.01$, *** = $p < 0.001$, ns = no significance, as determined by one-way ANOVA followed by a Tukey post-test.

Discussion

Impact of Polymer Length on Cargo Internalization

Lengthening homopolymer PTDMs beyond the 20 repeat units used in previous protein delivery studies did not improve internalization. This is likely because cationic homopolymer PTDMs generally bind proteins less effectively than their block copolymer counterparts.[9,29,40] Likewise, PTDMs with double the charge density had no appreciable advantage, suggesting that number of cations is perhaps less important for delivery of proteins than for nucleic acids.[35]

Block copolymer PTDMs were far more effective, though extending polymer length appeared to limit protein internalization. This reduction was more pronounced for EGFP delivery than for IgG-AF488 delivery. While it remains possible that protein denaturation contributed in part to the more dramatic reduction in EGFP delivery, the same trend was observed for IgG-AF488 delivery in two cell lines, supporting the hypothesis that many shorter PTDMs are more effective than fewer longer ones at maximizing cargo internalization.

Impact of Polymer Length on Cargo Activity

The opposite trend was observed when exploring the impact of polymer length on delivery of a functional protein, Cre recombinase. Gene recombination increased progressively with increasing carrier length, despite the presence of fewer individual polymer chains per molecule of Cre. It is interesting to note that **$MePh_{80}$-*b*-dG_{40}** was effective at a ratio of less than one polymer molecule per protein, whereas a large excess of polycation is almost always favorable, if not essential, for non-covalent delivery.[50–53]

Upon exploration of additional carrier:cargo ratios, the contrast between the different length PTDM was clear: for the conditions evaluated, **MePh$_{10}$-*b*-dG$_5$** was unable to facilitate any notable gene recombination whereas **MePh$_{80}$-*b*-dG$_{40}$** modified up to 60% of the cellular population. The 60% gene recombination achieved with this PTDM (at 125 nM Cre and 2.5:1 PTDM:Cre) compares favorably with our previous reports. In a recent study using the same reporter Jurkat T cell line, the polymers **MePh$_{10}$-*b*-dG$_5$**, **dMe$_{10}$-*b*-dG$_5$**, and **dPh$_5$-*b*-dG$_5$** yielded recombination rates of 25%, 50%, and 45%, respectively (560 nM, 5:1).[29] In a different human T cell line, **MePh$_9$-*b*-dG$_5$** reached 70% using Cre and 90% using a Tat-Cre conjugate, which facilitates some cellular entry on its own (125 nM, 10:1).[42] Two additional reports in this cell line demonstrated the abilities of **dPh$_5$-*b*-dG$_5$** and **dPh$_5$-*grad*-dG$_5$** (gradient architecture) to edit up to 70% (Cre) and 90% (Tat-Cre) of cells (100-150 nM, 5:1-10:1).[40,47] Finally, **dPh$_5$-*grad*-dG$_5$** was also used to deliver Tat-Cre into primary mouse T cells, reducing protein expression by approximately 50% (250 nM, ~5:1).[47] Cell type, polymer structure, and the Cre variant employed clearly impact delivery efficacy significantly. The variety of conditions summarized here attest to the robust activity of these PTDMs for Cre delivery, and the data in Figure 6 indicate that longer PTDMs enable more gene recombination at lower Cre and PTDM concentrations with minimal toxicity (125 nM, 2.5:1).

Impact of Polymer Length on Complexation

Polymer-protein binding studies revealed carrier-cargo association to be driven by the mass of polymer in the system (i.e., the molar ratio of polymer repeat units to protein molecules), rather than the number of individual polymer chains. Increasing carrier molecular weight while maintaining the mass of polymer in the system did not appear to significantly impact the tightness with which each carrier bound its cargo. Thus, the increased Cre activity observed when delivered with longer PTDMs was unlikely due to a weaker carrier-cargo association.

In contrast, carrier length substantially impacted particle size. The eight-fold increase in polymer size led to reductions in nanoparticle volume of one and four orders of magnitude, respectively, for Cre and IgG complexes. It is well known that the physicochemical properties of nanoparticles, including size, shape, charge, and surface chemistry, critically affect their internalization mechanism and efficiency, as well as ultimate subcellular distribution and cargo functionality.[50,54] Regarding size, both the total number and combined surface area of particles in solution are increased with decreasing volume, potentially influencing rates of particle internalization, complex disassembly, intracellular diffusion, or even activity of the cargo while remaining complexed at the particle surface.

Furthermore, complex size was highly dependent on PTDM concentration when using **$MePh_{10}$-*b*-dG_5**, consistent with past findings,[22,50] but independent of PTDM concentration when using **$MePh_{80}$-*b*-dG_{40}**. This implies that the two amphiphiles may form complexes with proteins via different mechanisms. The increased surfactant-like character of the longer PTDMs may impart greater stability to smaller complexes or even induce micellization. Complex size can impact myriad aspects of delivery, such as cellular internalization mechanism, endosomal escape, intracellular trafficking, and complex dissociation kinetics.[55–60] Thus, the use of longer PTDMs offers a convenient method for limiting the size of protein nanoparticles as well as boosting the IA of the delivered cargo.

Conclusions

Whereas siRNA cargoes can be adequately delivered with homopolymer PTDMs,[35] these polymers are poor protein carriers, regardless of polymer length, charge density, or anionic nature of the cargo. This is consistent with previous findings that the simple addition of a hydrophobic

block dramatically improves protein internalization.[29,40,41] Block copolymer degree of polymerization was found to affect protein delivery in competing ways. Although shortening these PTDMs maximized protein internalization, arranging the same number of monomers into fewer, longer polymer chains improved functional Cre delivery. This suggests that longer amphiphiles promote higher intracellular availability of their protein cargo even when minimal protein is delivered. Importantly, higher DP PTDMs with more surfactant-like character do not seem to significantly denature protein cargo. In contrast, they facilitate greater functional delivery. These longer PTDMs enabled 60% gene recombination at a lower carrier:cargo ratio of 2.5:1, implying that increased monomer connectivity enable mores effective cargo delivery with fewer total number of molecules.

In order to understand the cause of intracellular availability differences, carrier-cargo binding and complex size were studied. Measured carrier-cargo binding interactions were similar for various length PTDMs, however, complex size varied immensely. For PTDM:IgG complexes, particles ranged from 50 nm (DP = 120) to 1 μm (DP = 15) in diameter. Furthermore, unlike **MePh$_{10}$-*b*-dG$_5$** complexes, the size of **MePh$_{80}$-*b*-dG$_{40}$** complexes was independent of polymer concentration, indicating that they were particularly stable. While there is evidence in the literature of longer polymeric carriers protecting protein activity, the differences in intracellular availability seen here are likely due, at least in part, to differences in nanoparticle size. Cargoes contained within smaller nanoparticles may be more intracellularly available due to variations in cellular uptake mechanism, nanoparticle surface area, or release kinetics. It is also possible, however, that the structures of these polymer-protein assemblies are fundamentally different. Future studies will be necessary to more thoroughly characterize the complexation mechanism, nanoparticle structure, and potential micellization of these high molecular weight PTDMs.

Associated Content

Supporting Information

The Supporting Information is available free of charge on the RSC Publications website at DOI:

…

Materials and methods; supplemental delivery data; flow cytometry histograms; cellular viability; binding assays; dynamic light scattering (PDF)

Author Information

Corresponding Author

Gregory N. Tew – *Department of Polymer Science & Engineering, University of Massachusetts, Amherst, Massachusetts 01003, United States; Molecular and Cellular Biology Program, University of Massachusetts, Amherst, Massachusetts 01003, United States; Department of Veterinary & Animal Sciences, University of Massachusetts, Amherst, Massachusetts 01003, Untied States;* orcid.org/0000-0003-3277-7925
*Email: tew@mail.pse.umass.edu

Authors

Christopher R. Hango – *Department of Polymer Science & Engineering, University of Massachusetts, Amherst, Massachusetts 01003, United States;* orcid.org/0000-0002-4066-9548

Hazel C. Davis – *Department of Polymer Science & Engineering, University of Massachusetts, Amherst, Massachusetts 01003, United States;* orcid.org/0000-0003-3675-1650

Esha A. Uddin – *Department of Polymer Science & Engineering, University of Massachusetts, Amherst, Massachusetts 01003, United States*

Lisa M. Minter – *Molecular and Cellular Biology Program, University of Massachusetts, Amherst, Massachusetts 01003, United States; Department of Veterinary & Animal Sciences, University of Massachusetts, Amherst, Massachusetts 01003, Untied States;* orcid.org/0000-0002-1728-6389

Notes

The authors declare no competing financial interest.

Acknowledgements

This work was primarily supported by the National Science Foundation (NSF DMR-1308123) and the US Department of Defense (W81XWH1910540 and W81XWH2010536). C.R.H. and H.C.D. were partially supported by the US Department of Education Graduate Assistance in Areas of National Need Fellowship (DoED P200A150276). H.C.D. was additionally supported by the UMass Soft Materials for Life Sciences National Research Traineeship and Fellowship (NSF NRT-1545399) and a Spaulding Smith Diversity Fellowship through the Northeast Alliance for Graduate Education and Professoriate (NEAGAP) at UMass Amherst. The authors would like to thank Dr. Brittany deRonde and Ms. Leah Caffrey for help with polymer synthesis. Special thanks to Prof. Sandra L. Petersen for mHippoE-18 cells and Dr. Amy S. Burnside of the Flow Cytometry Core Facility at UMass Amherst.

References

(1) Deshayes, S.; Morris, M.; Heitz, F.; Divita, G. Delivery of proteins and nucleic acids using a non-covalent peptide-based strategy. *Adv. Drug Deliv. Rev.* **2008**, *60* (4–5), 537–547.

(2) Posey, N. D.; Tew, G. N. Associative and Dissociative Processes in Non-Covalent Polymer-Mediated Intracellular Protein Delivery. *Chem. - An Asian J.* **2018**, *13* (22), 3351–3365.

(3) Herrera Estrada, L. P.; Champion, J. A. Protein nanoparticles for therapeutic protein delivery. *Biomater. Sci.* **2015**, *3* (6), 787–799.

(4) González-Toro, D. C.; Thayumanavan, S. Advances in polymer and polymeric

nanostructures for protein conjugation. *Eur. Polym. J.* **2013**, *49* (10), 2906–2918.

(5) Pasut, G. Polymers for Protein Conjugation. *Polymers* **2014**, *6* (1), 160–178.

(6) Fu, A.; Tang, R.; Hardie, J.; Farkas, M. E.; Rotello, V. M. Promises and Pitfalls of Intracellular Delivery of Proteins. *Bioconjug. Chem.* **2014**, *25* (9), 1602–1608.

(7) Gong, Y.; Leroux, J. C.; Gauthier, M. A. Releasable Conjugation of Polymers to Proteins. *Bioconjugate Chemistry*. 2015, pp 1179–1181.

(8) Rao, J. P.; Geckeler, K. E. Polymer nanoparticles: Preparation techniques and size-control parameters. *Prog. Polym. Sci.* **2011**, *36* (7), 887–913.

(9) Davis, H. C.; Posey, N. D.; Tew, G. N. Protein Binding and Release by Polymeric Cell-Penetrating Peptide Mimics. *Biomacromolecules* **2022**, *23* (1), 57–66.

(10) Zhao, H.; Lin, Z. Y.; Yildirimer, L.; Dhinakar, A.; Zhao, X.; Wu, J. Polymer-based nanoparticles for protein delivery: design, strategies and applications. *J. Mater. Chem. B* **2016**, *4* (23), 4060–4071.

(11) Hamid Akash, M. S.; Rehman, K.; Chen, S. Natural and Synthetic Polymers as Drug Carriers for Delivery of Therapeutic Proteins. *Polym. Rev.* **2015**, *55* (3), 371–406.

(12) Bekale, L.; Agudelo, D.; Tajmir-Riahi, H. A. Effect of polymer molecular weight on chitosan–protein interaction. *Colloids Surfaces B Biointerfaces* **2015**, *125*, 309–317.

(13) Sabnis, S.; Block, L. H. Chitosan as an enabling excipient for drug delivery systems I. Molecular modifications. *Int. J. Biol. Macromol.* **2000**, *27*, 181–186.

(14) Long, J.; Xu, E.; Li, X.; Wu, Z.; Wang, F.; Xu, X.; Jin, Z.; Jiao, A.; Zhan, X. Effect of chitosan molecular weight on the formation of chitosan-pullulanase soluble complexes and their application in the immobilization of pullulanase onto Fe_3O_4-κ-carrageenan nanoparticles. *Food Chem.* **2016**, *202*, 49–58.

(15) Gan, Q.; Wang, T. Chitosan nanoparticle as protein delivery carrier—Systematic examination of fabrication conditions for efficient loading and release. *Colloids Surfaces B Biointerfaces* **2007**, *59* (1), 24–34.

(16) Xu, Y.; Du, Y. Effect of molecular structure of chitosan on protein delivery properties of chitosan nanoparticles. *Int. J. Pharm.* **2003**, *250* (1), 215–226.

(17) Janes, K. A.; Alonso, M. J. Depolymerized chitosan nanoparticles for protein delivery: Preparation and characterization. *J. Appl. Polym. Sci.* **2003**, *88* (12), 2769–2776.

(18) Wang, F.; Mo, J.; Huang, A.; Zhang, M.; Ma, L. Effects of interaction with gene carrier polyethyleneimines on conformation and enzymatic activity of pig heart lactate dehydrogenase. *Spectrochim. Acta - Part A Mol. Biomol. Spectrosc.* **2018**, *204*, 217–224.

(19) Guo, Z.; Kong, Z.; Wei, Y.; Li, H.; Wang, Y.; Huang, A.; Ma, L. Effects of gene carrier polyethyleneimines on the structure and binding capability of bovine serum albumin. *Spectrochim. Acta - Part A Mol. Biomol. Spectrosc.* **2017**, *173*, 783–791.

(20) Bekale, L.; Agudelo, D.; Tajmir-Riahi, H. A. The role of polymer size and hydrophobic end-group in PEG–protein interaction. *Colloids Surfaces B Biointerfaces* **2015**, *130*, 141–148.

(21) Jain, S.; Bates, F. S. On the origins of morphological complexity in block copolymer surfactants. *Science* **2003**, *300* (5618), 460–464.

(22) Posey, N. D.; Tew, G. N. Protein Transduction Domain Mimic (PTDM) Self-Assembly? *Polymers* **2018**, *10* (9), 1039.

(23) Reynhout, I. C.; Cornelissen, J. J. L. M.; Nolte, R. J. M. Synthesis of Polymer−Biohybrids: From Small to Giant Surfactants. *Acc. Chem. Res.* **2009**, *42* (6), 681–692.

(24) Mai, Y.; Eisenberg, A. Self-assembly of block copolymers. *Chem. Soc. Rev.* **2012**, *41* (18),

5969.

(25) Raffa, P.; Wever, D. A. Z.; Picchioni, F.; Broekhuis, A. A. Polymeric Surfactants: Synthesis, Properties, and Links to Applications. *Chem. Rev.* **2015**, *115* (16), 8504–8563.

(26) Shete, H. K.; Prabhu, R. H.; Patravale, V. B. Endosomal Escape: A Bottleneck in Intracellular Delivery. *J. Nanosci. Nanotechnol.* **2014**, *14* (1), 460–474.

(27) Xiang, S.; Tong, H.; Shi, Q.; Fernandes, J. C.; Jin, T.; Dai, K.; Zhang, X. Uptake mechanisms of non-viral gene delivery. *J. Control. Release* **2012**, *158* (3), 371–378.

(28) Khalil, I. A.; Kogure, K.; Akita, H.; Harashima, H. Uptake Pathways and Subsequent Intracellular Trafficking in Nonviral Gene Delivery. *Pharmacol. Rev.* **2006**, *58* (1), 32–45.

(29) Hango, C. R.; Backlund, C. M.; Davis, H. C.; Posey, N. D.; Minter, L. M.; Tew, G. N. Non-Covalent Carrier Hydrophobicity as a Universal Predictor of Intracellular Protein Activity. *Biomacromolecules* **2021**, *22* (7), 2850–2863.

(30) Frankel, A. D.; Pabo, C. O. Cellular uptake of the tat protein from human immunodeficiency virus. *Cell* **1988**, *55* (6), 1189–1193.

(31) Green, M.; Loewenstein, P. M. Autonomous functional domains of chemically synthesized human immunodeficiency virus tat trans-activator protein. *Cell* **1988**, *55* (6), 1179–1188.

(32) Vivès, E.; Brodin, P.; Lebleu, B. A Truncated HIV-1 Tat Protein Basic Domain Rapidly Translocates through the Plasma Membrane and Accumulates in the Cell Nucleus. *J. Biol. Chem.* **1997**, *272* (25), 16010–16017.

(33) Joliot, A.; Pernelle, C.; Deagostini-Bazin, H.; Prochiantz, A. Antennapedia homeobox peptide regulates neural morphogenesis. *Proc. Natl. Acad. Sci.* **1991**, *88* (5), 1864–1868.

(34) Derossi, D.; Joliot, A. H.; Chassaing, G.; Prochiantz, A. The third helix of the Antennapedia homeodomain translocates through biological membranes. *J. Biol. Chem.* **1994**, *269* (14),

10444–10450.

(35) Caffrey, L. M.; deRonde, B. M.; Minter, L. M.; Tew, G. N. Mapping Optimal Charge Density and Length of ROMP-Based PTDMs for siRNA Internalization. *Biomacromolecules* **2016**, *17* (10), 3205–3212.

(36) deRonde, B. M.; Torres, J. A.; Minter, L. M.; Tew, G. N. Development of Guanidinium-Rich Protein Mimics for Efficient siRNA Delivery into Human T Cells. *Biomacromolecules* **2015**, *16* (10), 3172–3179.

(37) deRonde, B. M.; Posey, N. D.; Otter, R.; Caffrey, L. M.; Minter, L. M.; Tew, G. N. Optimal Hydrophobicity in Ring-Opening Metathesis Polymerization-Based Protein Mimics Required for siRNA Internalization. *Biomacromolecules* **2016**, *17* (6), 1969–1977.

(38) Sarapas, J. M.; Backlund, C. M.; DeRonde, B. M.; Minter, L. M.; Tew, G. N. ROMP- and RAFT-Based Guanidinium-Containing Polymers as Scaffolds for Protein Mimic Synthesis. *Chem. - A Eur. J.* **2017**, *23* (28), 6858–6863.

(39) Backlund, C. M.; Sgolastra, F.; Otter, R.; Minter, L. M.; Takeuchi, T.; Futaki, S.; Tew, G. N. Increased hydrophobic block length of PTDMs promotes protein internalization. *Polym. Chem.* **2016**, *7* (48), 7514–7521.

(40) Sgolastra, F.; Backlund, C. M.; Ilker Ozay, E.; deRonde, B. M.; Minter, L. M.; Tew, G. N. Sequence segregation improves non-covalent protein delivery. *J. Control. Release* **2017**, *254*, 131–136.

(41) Backlund, C. M.; Takeuchi, T.; Futaki, S.; Tew, G. N. Relating structure and internalization for ROMP-based protein mimics. *Biochim. Biophys. Acta - Biomembr.* **2016**, *1858* (7), 1443–1450.

(42) Tezgel, A. Ö.; Jacobs, P.; Backlund, C. M.; Telfer, J. C.; Tew, G. N. Synthetic Protein

Mimics for Functional Protein Delivery. *Biomacromolecules* **2017**, *18* (3), 819–825.

(43) Backlund, C. M.; Parhamifar, L.; Minter, L.; Tew, G. N.; Andresen, T. L. Protein Transduction Domain Mimics Facilitate Rapid Antigen Delivery into Monocytes. *Mol. Pharm.* **2019**, *16* (6), 2462–2469.

(44) Ozay, E. I.; Gonzalez-Perez, G.; Torres, J. A.; Vijayaraghavan, J.; Lawlor, R.; Sherman, H. L.; Garrigan, D. T.; Burnside, A. S.; Osborne, B. A.; Tew, G. N.; Minter, L. M. Intracellular Delivery of Anti-pPKCθ (Thr538) via Protein Transduction Domain Mimics for Immunomodulation. *Mol. Ther.* **2016**, *24* (12), 2118–2130.

(45) Ozay, E. I.; Shanthalingam, S.; Sherman, H. L.; Torres, J. A.; Osborne, B. A.; Tew, G. N.; Minter, L. M. Cell-Penetrating Anti-Protein Kinase C Theta Antibodies Act Intracellularly to Generate Stable, Highly Suppressive Regulatory T Cells. *Mol. Ther.* **2020**, *28* (8), 1987–2006.

(46) Ozay, E. I.; Shanthalingam, S.; Torres, J. A.; Osborne, B. A.; Tew, G. N.; Minter, L. M. Protein Kinase C Theta Modulates PCMT1 through hnRNPL to Regulate FOXP3 Stability in Regulatory T Cells. *Mol. Ther.* **2020**, *28* (10), 1–17.

(47) Sgolastra, F.; Kuksin, C. A. A.; Gonzalez-Perez, G.; Minter, L. M.; Tew, G. N. Enhanced TAT-Cre Protein Transduction for Efficient Gene Recombination in T cells. *ACS Appl. Bio Mater.* **2018**, *1*, 444–451.

(48) Posey, N. D.; Caffrey, L. M.; Minter, L. M.; Tew, G. N. Protein Mimic Hydrophobicity Affects Intracellular Delivery but not Cargo Binding. *ChemistrySelect* **2016**, *1* (19), 6146–6150.

(49) Posey, N. D.; Hango, C. R.; Minter, L. M.; Tew, G. N. The Role of Cargo Binding Strength in Polymer-Mediated Intracellular Protein Delivery. *Bioconjug. Chem.* **2018**, *29* (8), 2679–

2690.

(50) Muñoz-Morris, M. A.; Heitz, F.; Divita, G.; Morris, M. C. The peptide carrier Pep-1 forms biologically efficient nanoparticle complexes. *Biochem. Biophys. Res. Commun.* **2007**, *355* (4), 877–882.

(51) Sahay, G.; Alakhova, D. Y.; Kabanov, A. V. Endocytosis of nanomedicines. *J. Control. Release* **2010**, *145* (3), 182–195.

(52) Ballarín-González, B.; Howard, K. A. Polycation-based nanoparticle delivery of RNAi therapeutics: Adverse effects and solutions. *Adv. Drug Deliv. Rev.* **2012**, *64* (15), 1717–1729.

(53) Thibault, M.; Astolfi, M.; Tran-Khanh, N.; Lavertu, M.; Darras, V.; Merzouki, A.; Buschmann, M. D. Excess polycation mediates efficient chitosan-based gene transfer by promoting lysosomal release of the polyplexes. *Biomaterials* **2011**, *32* (20), 4639–4646.

(54) Shang, L.; Nienhaus, K.; Nienhaus, G. Engineered nanoparticles interacting with cells: size matters. *J. Nanobiotechnology* **2014**, *12* (1), 5.

(55) Kettler, K.; Veltman, K.; van de Meent, D.; van Wezel, A.; Hendriks, A. J. Cellular uptake of nanoparticles as determined by particle properties, experimental conditions, and cell type. *Environ. Toxicol. Chem.* **2014**, *33* (3), 481–492.

(56) Yameen, B.; Choi, W. Il; Vilos, C.; Swami, A.; Shi, J.; Farokhzad, O. C. Insight into nanoparticle cellular uptake and intracellular targeting. *J. Control. Release* **2014**, *190*, 485–499.

(57) Selby, L. I.; Cortez-Jugo, C. M.; Such, G. K.; Johnston, A. P. R. Nanoescapology: progress toward understanding the endosomal escape of polymeric nanoparticles. *Wiley Interdiscip. Rev.: Nanomed. Nanobiotechnol.* **2017**, *9* (5), e1452.

(58) Smith, S. A.; Selby, L. I.; Johnston, A. P. R. R.; Such, G. K. The Endosomal Escape of Nanoparticles: Toward More Efficient Cellular Delivery. *Bioconjug. Chem.* **2019**, *30* (2), 263–272.

(59) Yus, C.; Irusta, S.; Sebastian, V.; Arruebo, M. Controlling Particle Size and Release Kinetics in the Sustained Delivery of Oral Antibiotics Using pH-Independent Mucoadhesive Polymers. *Mol. Pharm.* **2020**, *17* (9), 3314–3327.

(60) Guo, X.; Wei, X.; Chen, Z.; Zhang, X.; Yang, G.; Zhou, S. Multifunctional nanoplatforms for subcellular delivery of drugs in cancer therapy. *Prog. Mater. Sci.* **2020**, *107*, 100599.